Molecular Microbiology (2010) 76(2), 489–502

doi:10.1111/j.1365-2958.2010.07116.x
First published online 30 March 2010

Shear-enhanced binding of intestinal colonization factor antigen I of enterotoxigenic *Escherichia coli*

Veronika Tchesnokova,[1] Annette L. McVeigh,[2] Brian Kidd,[3] Olga Yakovenko,[3] Wendy E. Thomas,[3] Evgeni V. Sokurenko[1] and Stephen J. Savarino[2,4]***

Departments of [1]Microbiology and [3]Engineering, University of Washington, Seattle, WA 98195-7242, USA.

[2]Enteric Diseases Department, Naval Medical Research Center, 503 Robert Grant Avenue, Silver Spring, MD 20910-7500, USA.

[4]Department of Pediatrics, Uniformed Services University of the Health Sciences, Bethesda, MD 20814, USA.

Summary

In the intestine, enterotoxigenic *Escherichia coli* works against peristaltic forces, adhering to the epithelium via the colonization factor antigen I (CFA/I) fimbrial adhesin CfaE. The CfaE adhesin is similar in localization and tertiary (but not primary) structure to FimH, the type 1 fimbrial adhesin of uropathogenic *E. coli*, which shows shear-dependent binding to epithelial receptors by an allosteric catch-bond mechanism. Thus, we speculated that CfaE is also capable of shear-enhanced binding. Indeed, bovine erythrocytes coursing over immobilized CFA/I fimbriae in flow chambers exhibited low accumulation levels and fast rolling at low shear, but an 80-fold increase in accumulation and threefold decrease in rolling velocity at elevated shear. This effect was reversible and abolished by pre-incubation of fimbriae with anti-CfaE antibody. Erythrocytes bound to whole CfaE in the same shear-enhanced manner, but to CfaE adhesin domain in a shear-inhibitable fashion. Residue replacements designed to disrupt CfaE interdomain interaction decreased the shear dependency of adhesion and increased binding under static conditions to human intestinal epithelial cells. These findings indicate that close interaction between adhesive and anchoring pilin domains of CfaE keeps the former in a low-affinity state that toggles into a high-affinity state upon separation of two domains, all consistent with an allosteric catch-bond mechanism of CfaE binding.

Accepted 24 February, 2010. For correspondence. *E-mail stephen.savarino@med.navy.mil; Tel. (+1) 301 319 7650; Fax (+1) 301 319 7679; **E-mail evs@u.washington.edu; Tel (+1) 206 685 2162; Fax (+1) 206 543 8297.

Introduction

Many pathogenic microorganisms express fimbriae (or pili), polymeric protein appendages that extend from the bacterial surface. Fimbriae often attach to specific host-cell receptors to promote colonization, a decisive early step in infection. Enterotoxigenic *Escherichia coli* (ETEC), a major cause of human and veterinary diarrhea, express fimbriae to facilitate small intestinal colonization and produce enterotoxins that cause electrolyte and fluid secretion (Levine, 1987; Gaastra and Svennerholm, 1996). A variety of human-specific ETEC colonization factors have been described, the first of which was colonization factor antigen I (CFA/I) fimbriae (Evans *et al.*, 1975). CFA/I plays a critical role in pathogenesis, induces a protective immune response and is also archetypal of the largest genetically related class of ETEC fimbriae (Freedman *et al.*, 1998; Gaastra *et al.*, 2002). These so-called class 5 fimbriae comprise eight discrete sub-types associated with human ETEC, which share common structural and biogenesis features (Anantha *et al.*, 2004).

Colonization factor antigen I fimbriae are constructed by the alternate chaperone pathway, requiring a periplasmic chaperone (CfaA) and an outer membrane usher (CfaC) (Jordi *et al.*, 1992; Sakellaris *et al.*, 1996). These auxiliary components orchestrate the formation of a heteropolymeric, hair-like structure on the bacterial surface that contains CfaE, the tip-localized minor subunit and major subunit CfaB. CFA/I fimbriae are genetically and functionally distinguished from fimbriae assembled by the classical chaperone-usher pathway (e.g. mannose-specific type 1 and di-galactose-specific P fimbriae), although they bear morphological resemblance (Mu *et al.*, 2008). Like type 1 and P fimbriae, CFA/I exploit the donor–strand complementation and exchange mechanism in the bioassembly process, wherein the structural protein subunits are folded into immunoglobulin-like β-sandwich domains, and the N-terminal β-strand from one subunit is inserted into a groove formed in the preceding subunit by a missing β-strand (Li *et al.*, 2007; Poole *et al.*, 2007).

Report Documentation Page

Form Approved
OMB No. 0704-0188

1. REPORT DATE	2. REPORT TYPE	3. DATES COVERED
FEB 2010		**00-00-2010 to 00-00-2010**

4. TITLE AND SUBTITLE	5a. CONTRACT NUMBER
Shear-enhanced binding of intestinal colonization factor antigen I of enterotoxigenic Escherichia coli	5b. GRANT NUMBER
	5c. PROGRAM ELEMENT NUMBER
6. AUTHOR(S)	5d. PROJECT NUMBER
	5e. TASK NUMBER
	5f. WORK UNIT NUMBER
7. PERFORMING ORGANIZATION NAME(S) AND ADDRESS(ES) **Naval Medical Research Center,Enteric Diseases Department,503 Robert Grant Avenue,Silver Spring,MD,20910**	8. PERFORMING ORGANIZATION REPORT NUMBER
9. SPONSORING/MONITORING AGENCY NAME(S) AND ADDRESS(ES)	10. SPONSOR/MONITOR'S ACRONYM(S)
	11. SPONSOR/MONITOR'S REPORT NUMBER(S)

12. DISTRIBUTION/AVAILABILITY STATEMENT
Approved for public release; distribution unlimited

13. SUPPLEMENTARY NOTES

14. ABSTRACT

15. SUBJECT TERMS

16. SECURITY CLASSIFICATION OF:			17. LIMITATION OF ABSTRACT	18. NUMBER OF PAGES	19a. NAME OF RESPONSIBLE PERSON
a. REPORT **unclassified**	b. ABSTRACT **unclassified**	c. THIS PAGE **unclassified**	**Same as Report (SAR)**	**14**	

The natural substrate to which CFA/I fimbriae adhere is found on the human small intestinal surface. Demonstration that CFA/I also induces mannose-resistant haemagglutination (MRHA) of human, bovine and chicken erythrocytes led to the adoption of this assay as a proxy model for the study of CFA/I adhesion (Evans *et al.*, 1979). Evidence suggests that a sialylated glycoprotein serves as the eukaryotic receptor, although a specific enterocyte or red cell receptor remains to be identified (Evans *et al.*, 1979; Bartus *et al.*, 1985). The minor, tip-associated subunit CfaE has been clearly ascribed a direct role in both erythrocyte and human enterocyte adherence and, thus, is viewed as the key fimbrial adhesive subunit (Li *et al.*, 2007; Poole *et al.*, 2007; Baker *et al.*, 2009).

As with many other bacterial adhesins, CFA/I fimbriae are presumed to establish and maintain binding to target cells in the face of hydrodynamic shear forces, in this case generated by peristaltic activity in the gastrointestinal tract. It has generally been assumed that shear stress inhibits pathogen adhesion, thereby serving as a non-specific host defense against bacterial colonization. Recently, however, a novel mode of shear-enhanced, or so-called catch-bond, adhesion has been described in bacteria wherein the adhesive interactions become stronger rather than weaker under increasing shear conditions (Thomas *et al.*, 2002; 2004). The principle and mechanism of catch-bond formation has been discovered and extensively studied using type 1 fimbriae of *E. coli* as the model. FimH, the type 1 adhesive subunit, is positioned at the fimbrial tip, similar to the localization of the CfaE adhesin of CFA/I fimbriae. Whereas type 1 fimbriae bind weakly to mannosylated surfaces under static conditions, the introduction of shear stress by increasing the flow of a bacterial suspension over the surface switches the interaction from weak, rolling bacterial adhesion to strong binding with cessation of bacterial movement at forces between 1 and 10 dynes cm^{-2} (or 10 and 100 $\mu N\ cm^{-2}$) (Thomas *et al.*, 2004).

In our working model for catch-bond formation, the mannose binding lectin domain of FimH can either interact with or be separated from the fimbria-anchoring pilin domain of FimH, and the latter allosterically controls the conformational and functional state of the lectin domain (Tchesnokova *et al.*, 2008; Yakovenko *et al.*, 2008). When the two domains interact under no or low shear, the distal mannose binding pocket assumes a low-affinity conformation. The domains separate under increasing shear, and in so doing convert the lectin domain into a high-affinity conformation. Besides application of force across the mannose-FimH bond, other conditions can lock FimH in the high-affinity state, such as the introduction of mutations that disrupt interdomain interactions and the insertion of wedging molecules (e.g. antibodies against the interdomain interface epitopes) that sterically lever open the interface (Aprikian *et al.*, 2007; Tchesnokova *et al.*, 2008). Such shear-enhanced binding appears to benefit microbial colonization by reducing susceptibility of adherent bacteria to soluble inhibitors, facilitating surface spread of bacterial biofilms, and possibly conferring other advantages as well (Nilsson *et al.*, 2006a; Anderson *et al.*, 2007).

Its solved structure indicated that CfaE has a two-domain architecture, similar to FimH (Li *et al.*, 2007). CfaE was crystallized in the form of a variant containing a C-terminal extension comprising the donor β-strand from the CfaB major subunit, which compensates for the missing seventh strand of the CfaE pilin domain. In contrast, the FimH crystal structure was obtained in complex with its molecular chaperone (FimC), which is wedged between the two FimH domains. As has been predicted for the structure of FimH in the absence of its chaperone, the two CfaE domains interact closely with one another, and this close interface may set CfaE up to form an allosterically regulated catch bond with its putative receptor. Heretofore, however, no studies have been undertaken to determine the relationship between shear and adhesion for CFA/I fimbriae. In fact, type 1 fimbriae and FimH constitute the only bacterial system for which the structural aspects of catch-bond formation have been explored in detail.

Here we exploit the model of CFA/I-mediated binding to red blood cells (RBCs) under controlled flow conditions to demonstrate that CfaE-mediated binding is indeed shear-enhanced. Our findings are consistent with a catch-bond mechanism of CfaE binding to eukaryotic receptors, providing a novel functional and structural model for understanding the physiological significance and molecular details of shear-enhanced adhesion.

Results

Purified CFA/I fimbriae exhibit shear-dependent binding to erythrocytes

To test whether CFA/I fimbriae mediate shear-enhanced binding, purified fimbriae were adsorbed to the polystyrene plate of a parallel plate flow chamber (PPFC). A suspension of bovine RBCs was then loaded into the chamber, allowed to settle and then subjected to flow under various shear forces. The extent of bovine erythrocyte binding to the fimbrial carpet at different shear forces was determined by measurement of: (i) erythrocyte accumulation on the fimbriae-adsorbed surface (i.e., the relative proportion of erythrocytes that remained stationary or rolling at rates below the hydrodynamic velocity) and (ii) the average velocity of surface-bound erythrocytes.

At low shear forces (i.e., between 0.1 and 0.5 dynes cm^{-2}), bovine erythrocyte accumulation was

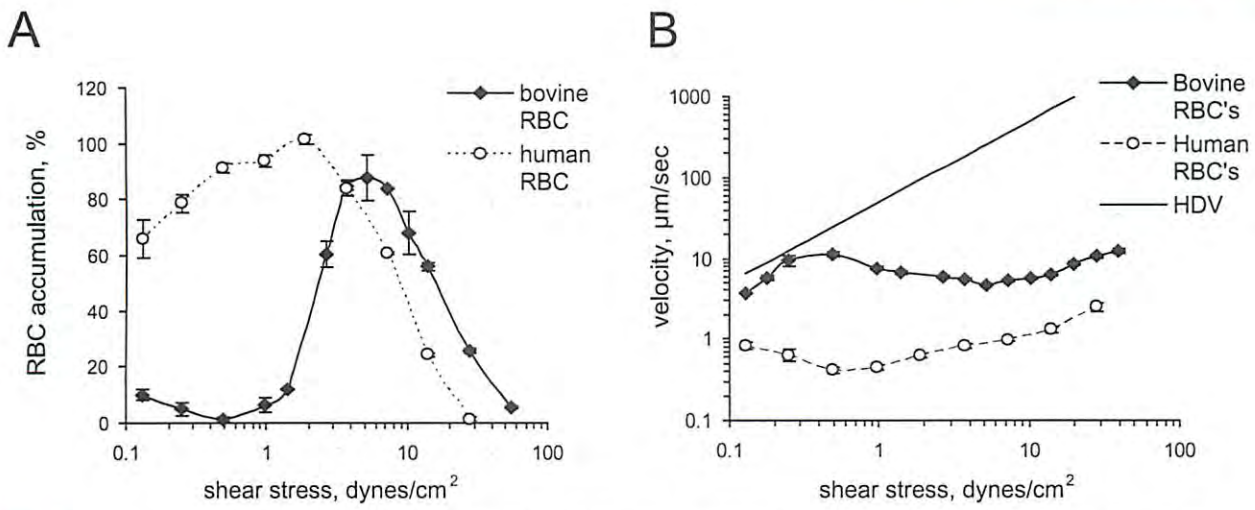

Fig. 1. Bovine RBCs binding to wild-type CFA/I fimbriae in PPFC. Fimbriae were immobilized on the surface of the flow chamber, RBCs were loaded, allowed to settle, and then the flow was turned on at various shear stress.
A. Erythrocytes at the surface, which are moving slower then the free-floating cells, were enumerated for all shear stress values and divided by the initial number of cells to calculate the percentage. Error bars represent standard deviation of bound erythrocytes throughout the recorded video.
B. The average velocity of bound erythrocytes was measured for every shear stress. Error bars represent the standard deviation of velocity measured for 100 single cells. HDV – hydrodynamic velocity, determined empirically for RBCs moving at the surface, but not bound to it. All experiments were performed at least twice on different plates with same results. As a negative control, same set of experiments was performed on BSA-quenched plates without immobilized CFA/I fimbriae. Here, no slowing of erythrocytes on the surface was observed; all the cells were moving with hydrodynamic velocity (data not shown).

relatively low. The proportion of red cells remaining on the surface decreased from 11% at the lowest shear to 1% at 0.5 dynes cm^{-2}. The corresponding velocity of bound bovine erythrocytes showed a gradual increase as shear force rose over this range (Fig. 1). Thus, in this low shear range, fimbriae–erythrocyte interactions were weak and exhibited a pattern consistent with shear inhibition rather than shear enhancement. With a further, stepwise increase in shear up to 5 dynes cm^{-2}, however, bovine erythrocyte accumulation increased up to 90% and was paralleled by a more than threefold decrease in erythrocyte velocity (Fig. 1). Hence, in this intermediate shear range (i.e., 0.5–5.0 dynes cm^{-2}) CFA/I fimbriae manifest shear-enhanced binding to its erythrocyte receptor. At 5.0 dynes cm^{-2}, bovine erythrocyte accumulation was almost 10-fold higher than that observed at the lowest shear values tested or more than 80-fold higher than at 0.5 dynes cm^{-2} where the weakest adhesion level was observed. Correspondingly, bovine erythrocyte velocity showed similar values despite nearly a 40-fold shear increase (i.e., from 0.13–5.0 dynes cm^{-2}). Notably, further increases in shear resulted in a gradual lowering of bovine erythrocyte accumulation and an increase in their velocity.

Similar experiments to those described above were conducted using human in place of bovine erythrocytes to determine if shear-enhanced binding of CFA/I to a presumably distinct but related receptor is evident. Indeed, the pattern of shear enhancement was observed (Fig. 1). The absolute changes in erythrocyte accumulation and velocity were less marked but still significant ($P < 0.0001$) with human erythrocytes, owing to stronger interaction between CFA/I fimbriae and human erythrocytes under the lowest shear stress conditions tested. The curve of erythrocyte accumulation showed a modest leftward shift in its peak for human versus bovine erythrocytes and in the low range of shear stress (i.e., < 0.5 dyne cm^{-2}) shear-inhibitable binding was not observed with human erythrocytes. The different shear-dependent binding pattern for human erythrocytes apparently is the result of differences in the kinetics of CFA/I fimbriae interaction with the human RBC receptor (see *Discussion*).

Taken together, the interaction between CFA/I fimbriae and both bovine and human erythrocytes is indicative of a shear-enhanced binding mode. Because this relationship was more pronounced for CFA/I–bovine erythrocyte interactions, bovine erythrocytes were used in all subsequent experiments.

We next examined reversibility of the CFA/I shear-enhanced binding phenotype. Bovine erythrocytes were allowed to settle in the flow chamber and then exposed to a constant shear stress near peak binding levels (3.7 dynes cm^{-2}). At set intervals, the shear stress was abruptly lowered to 0.13 dynes cm^{-2} and then returned to 3.7 dynes cm^{-2}. The proportion of erythrocytes bound to the fimbrial carpet diminished during each successive low shear pulse, dropping to 2% accumulation by the end of

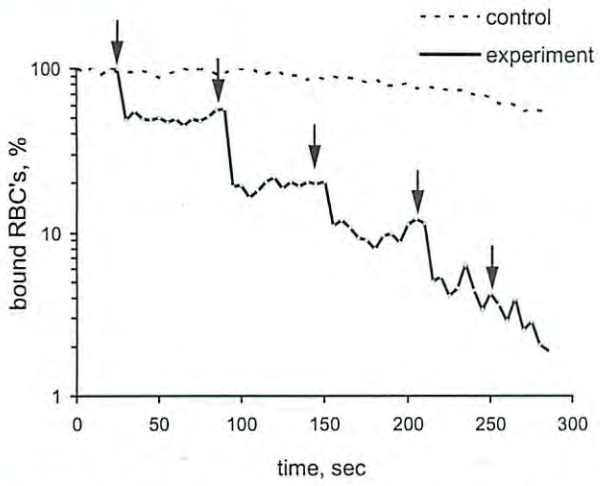

Fig. 2. Binding of RBCs to immobilized CFA/I fimbriae at high shear is reversible. The PPFC surface was coated with wild-type CFA/I fimbriae, bovine RBCs were loaded in the flow chamber, settled down, and then the flow was turned to 3.7 dynes cm^{-2} to bind them to fimbriae. The flow was either kept at 3.7 dynes cm^{-2} for 5 min (control line), or was occasionally turned down to 0.13 dynes cm^{-2} for 10 s (shown by arrows), and then back to 3.7 dynes cm^{-2} (experiment line). This experiment was performed several times on different plates with the same results.

the observation period (Fig. 2, solid line). To contrast, in control flow chambers where shear stress was constantly maintained, over 50% of erythrocytes remained bound to the fimbrial carpet (Fig. 2, dotted line). These findings indicate that CFA/I-mediated shear-enhanced binding to bovine erythrocytes is fully reversible, suggesting dynamic conformational changes in the adhesin structure and function, rather than a mere increase in the bond number under shear.

Shear-dependent erythrocyte binding of CFA/I fimbriae is attributable to CfaE

The weight of prior evidence suggests that the minor, tip-localized subunit CfaE functions as the CFA/I fimbrial adhesin (Li *et al.*, 2007; Poole *et al.*, 2007; Baker *et al.*, 2009). We therefore assessed whether CFA/I shear-enhanced bovine erythrocyte binding is attributable to CfaE. Pre-incubation of the fimbrial carpet with anti-CfaE MAb P10A7 abolished erythrocyte accumulation over the entire range of shear forces studied (Fig. 3A).

Experiments were also conducted in which unaltered CFA/I fimbriae were replaced with fimbriae containing CfaE into which individual point mutations had been introduced in the putative receptor binding pocket that repress MRHA (Li *et al.*, 2007). Interactions between bovine erythrocytes and fimbrial carpets containing any one of these altered CFA/I fimbriae did not exhibit a shear-enhanced binding phenotype (Fig. 3B). Interestingly, in comparison with the wild-type fimbriae, the binding pocket mutations increased accumulation of bovine erythrocytes at the lowest flow. It is possible that this binding is non-specific (as seen with bovine erythrocytes to a BSA-coated flow chamber – data not shown) or a novel ligand specificity acquired by the mutants. However, as the actual CfaE receptor and the exact binding pocket location is unknown at this time, we can only speculate about the nature of increased binding under low shear.

Finally, in chambers to which purified dscCfaE (*in cis* donor–strand complemented CfaE) had been adsorbed to the floor, the relationship between bovine erythrocyte accumulation and shear stress showed a bimodal distribution similar to that observed with native CFA/I fimbriae (Fig. 4A). Moreover, pretreatment of CfaE-coated chamber plates with the anti-CfaE MAb P10A7 resulted in abolition of all erythrocyte binding (data not shown). Taken together, these findings indicate that CfaE is largely responsible for CFA/I-mediated shear-dependent binding phenotype.

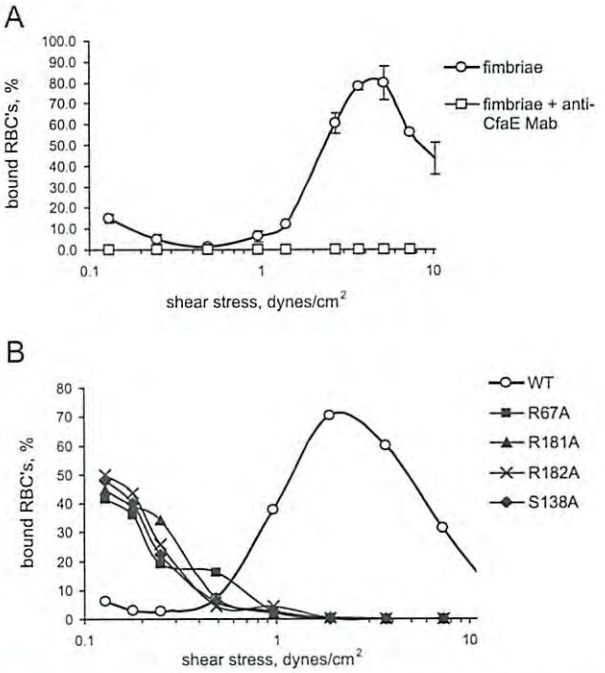

Fig. 3. Shear-enhanced binding of bovine RBCs by CFA/I fimbriae is promoted by minor subunit, CfaE.
A. Anti-CfaE monoclonal antibodies inhibit shear-enhanced binding. Wild-type CFA/I fimbriae were immobilized on the surface and incubated with anti-CfaE monoclonal antibodies. Then binding of erythrocytes at various shear stresses was determined.
B. Point mutations in the putative CfaE receptor binding domain abolish shear-enhanced binding of mutant CFA/I fimbriae. CFA/I fimbriae harbouring wild-type (WT) or mutant CfaE adhesin were immobilized on the surface. Binding of erythrocytes at the range of shear stress values was then determined. Peak binding was observed at a shear stress of 1.9 dynes cm^{-2}.

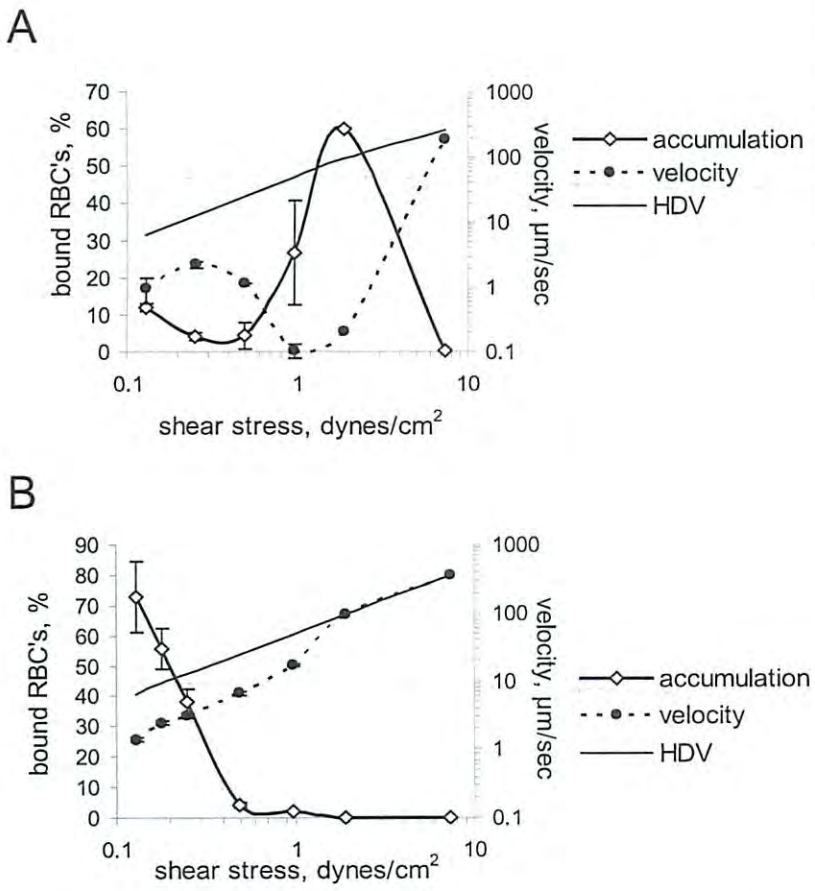

Fig. 4. Different modes of RBC binding to immobilized full-length minor subunit dscCfaE (A) or the adhesin domain truncate, CfaEad (B). Purified proteins were immobilized on the surface, RBCs were loaded into PPFC, settled down, and the flow was turned to various shears. Accumulation of RBCs at each shear value was recorded (solid line with open diamonds), and average velocity of bound RBCs was determined (dotted line with closed circles). HDV, hydrodynamic velocity (solid line).

Pilin domain regulates the CfaE-mediated shear-enhanced adhesion

To test whether the CfaE adhesin domain (CfaEad), in the absence of the CfaE pilin domain (CfaEpd), manifests shear-enhanced binding to bovine erythrocytes, purified CfaEad was immobilized in the flow chamber. At the lowest shear forces, a high proportion of erythrocytes were bound to the CfaEad-coated surface, with 70% red cell accumulation at 0.13 dynes cm^{-2} (Fig. 4B). This binding was completely inhibited by pretreatment with anti-CfaE MAb P10A7 (data not shown). With further increase in shear stress, however, this accumulation progressively diminished, with little to no accumulation detected at shear stress above 0.5 dynes cm^{-2}. Hence, isolated from the pilin domain, CfaEad exhibited strong binding to bovine erythrocytes at low shear stress level, and this interaction showed a unimodal pattern of shear inhibition rather than shear enhancement when shear stress was increased.

To assess the role of CfaE interdomain interactions in shear-enhanced binding, CFA/I fimbriae containing CfaE point mutations predicted to disrupt this interface were generated. In total, there are 17 hydrogen bonds between residues on either side of this interface (Fig. 5, and Li *et al.*, 2007). Of note, CfaE-G168 on the adhesin domain face participates in four H-bonds to F240, S244 and L325 on the pilin domain facing. A short 3/10-helix buried in the pilin domain (i.e., K201-G202-N203) serves as the linker connecting the two domains. Evaluated point mutations included ones that disrupted three or more of the aforementioned H-bonds, namely, G168A and G168D, S244N and S244G, and K201P, the latter also disrupting secondary structure of the interdomain linker.

Purified CFA/I fimbriae harbouring mutant CfaE were adsorbed to the chamber floor, and flow experiments were conducted to assess bovine erythrocyte binding to each. Certain mutations, such as CfaE-S244G and CfaE-G168A, did not significantly alter the binding pattern (Fig. 6A). Notable changes were observed with CfaE-K201P and CfaE-S244N, including a broadening of the bell curve and an elevated erythrocyte accumulation at relatively lower shear stress (Fig. 6A). For example, at 0.5 dynes cm^{-2} shear, erythrocyte accumulations of 15%, 59% and 66% were observed on fimbrial carpets that incorporated CfaE wild type, CfaE-K201P and CfaE-S244N respectively. These findings suggest that for these particular mutations, the switch from weak to strong

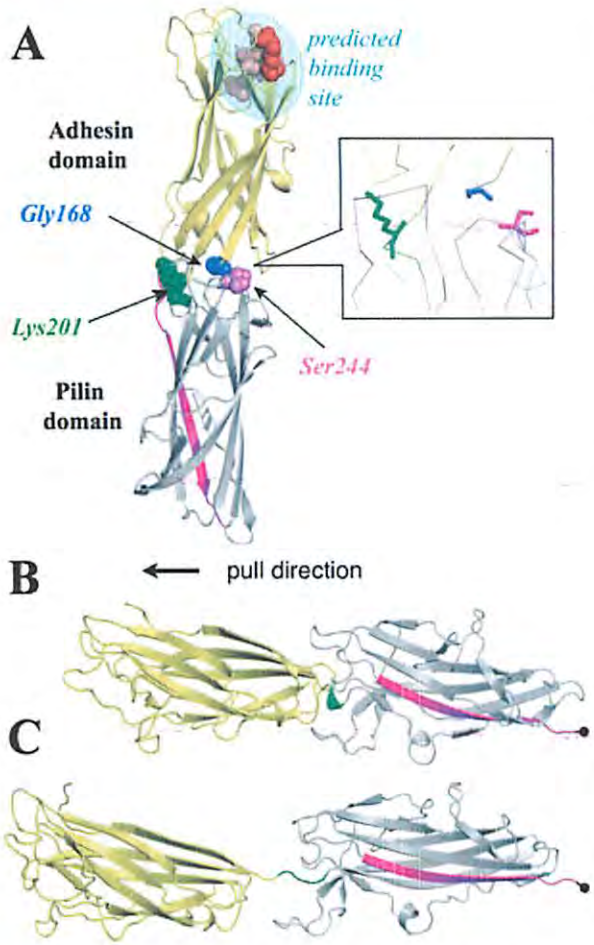

Fig. 5. Adhesin and pilin domains of CfaE subunit can separate via linker chain extension mechanism.
A. The crystal structure of CfaE is shown, with the following colour key: adhesin domain is shown in gold, pilin domain in silver, linker chain in green, donor strand in magenta. The putative binding site residues Arg67, Ser138, Arg182 are shown in pink while Arg181 is in red. Selected residues participating in interdomain interaction are shown as Gly168, blue; Lys201, green; and Ser244, purple. Blowout shows close-up view of interdomain region.
B. and C. Domain separation and extension of the linker chain in CfaE protein during steered molecular dynamics simulation. At the beginning of the simulation, the adhesin domain is in direct contact with the pilin domain and the linker chain (green) is coiled into a 3/10-helix. Application of mechanical force to the adhesin domain's centre of mass while holding the C-terminus (black sphere) of the self-complementing donor strand (magenta) fixed, causes the domains to separate and the linker chain to extend. Images of protein structures were generated with PyMOL.

binding is more exquisitely sensitive to shear stress than for unmodified CfaE. The most prominent effect on erythrocyte binding was observed with the CfaE-G168D mutant, which is predicted to disrupt four hydrogen bonds at the interface. Although bacteria expressed fewer CfaE-G168D fimbriae than wild type (possibly because of the disrupted fimbrial biogenesis; Fig. S1A), after adjusting the amount of purified immobilized fimbriae a significant elevation in bovine erythrocyte accumulation over wild-type CFA/I was detectable with the mutant fimbriae at the lowest shear stress levels (0.13–0.2 dynes cm^{-2}, see Fig. 6A). As shear stress levels were increased, erythrocyte accumulation diminished sharply to the point where no binding was detectable at or above 1.9 dynes cm^{-2} (Fig. 6A). Correspondingly, erythrocyte velocity over the CfaE/G168D modified fimbrial carpet was less than that over wild-type fimbriae at the lowest shears but steadily rose as shear stress was increased (Fig. 6B). To be sure, erythrocyte binding to this CfaE mutant most closely resembled that to CfaEad rather than to wild-type fimbriae or the two-domain dscCfaE. All binding was completely inhibited by pretreatment with MAb P10A7 (data not shown).

The findings described above demonstrate that CfaEad must be natively apposed to the pilin domain to achieve weak binding under low shear conditions. This is consistent with the hypothesis that interactions between domains regulate the switch from a low- to high-affinity conformation of the adhesin with the shear increase. The effect the mutations in CfaE had on the bell-like binding curve is similar to the previously described mutations in FimH that lead to increased affinity of FimH adhesin towards mannose (Weissman *et al.*, 2007). There, the affinity-increasing mutations that had a relatively low or moderate effect on binding at the lowest shear (like K201P and S244N for CfaE in this case) also caused an increased level of binding at all shears, including high shears, broadening the binding curve. Such mutations are thought to increase overall affinity not only (or as much) by increased frequency of the high-affinity state of the adhesin in intact fimbriae, but also (or primarily) by facilitating the switch from low- to high-affinity state under tensile force upon the binding initiation. In contrast, mutations that lead to the dominance of high-affinity state even without application of tensile force display a shear-inhibitable non-bell-like binding curve, where binding at higher shear for the mutant adhesin is lower than for the wild type (like G168D in CfaE). The likely explanation for this phenomenon is the decrease in the on-rate of binding when the adhesin is constantly in a high-affinity conformation.

Extension of the interdomain linker chain allows for separation between the binding and pilin domains

According to the crystal structure of CfaE, its adhesin and pilin domains closely interact with one another. The buried surface area between domains is nearly 700 A^2, and the short linker chain (3/10-helix consisting of three amino acids) is buried in the pilin domain, so that the whole protein assumes a cylindrical form (Li *et al.*, 2007). To determine whether the domains can potentially be separated under external force without major disruptions in

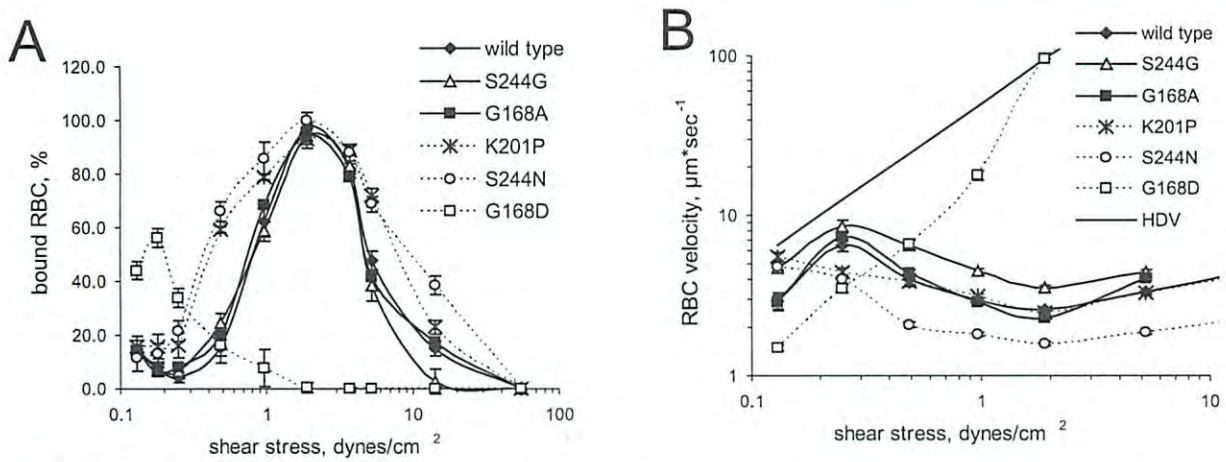

Fig. 6. Mutations predicted to diminish interactions between the adhesin and pilin domains of CfaE affect shear-enhanced binding of erythrocytes to immobilized mutant fimbriae.
A. RBCs binding over the range of shear stresses in PPFC to immobilized fimbriae harbouring wild-type and mutant CfaE adhesins.
B. Velocities of bound RBCs from (A).

protein integrity, we used steered molecular dynamics (SMD) to pull on the centre of mass of the adhesin domain while holding the C-terminus fixed (Fig. 5B and C and Video S1). The SMD simulation showed that, upon application of tensile force, the buried 3/10-helix linker chain uncoils, resulting in extension of the linker by 10 angstroms. The linker chain extension and domain separation occurred concomitantly, with an increase in the interdomain interaction energy, from –150 to 0 kcal mol^{-1}, suggesting that the two domains have lost all meaningful contacts and are no longer interacting. Thus, uncoiling of the pilin domain-buried linker chain appears to lead to linker extension, which in turn allows full separation between the adhesin and pilin domains of CfaE.

Interdomain CfaE mutations increase binding to human epithelial cells

To determine the potential relevance of shear-dependent binding of CfaE in bacterial interaction with human intestinal epithelium, we used the human intestinal cell line, Caco-2, shown to bind CFA/I fimbriated bacteria (Darfeuille-Michaud *et al.*, 1990). Unfortunately, the Caco-2 cell monolayer was not stable enough to withstand the sufficiently long shear stress levels used in our assays, which precluded meaningful assessment of Caco-2/bacterial binding in the flow chamber. Under static conditions, to obtain measurable adhesion levels of bacteria expressing the wild-type CfaE, a 2.5×10^8 cfu ml^{-1} bacterial suspension was incubated with Caco-2 cells for 3 h (Figs 7, S2A and B), indicating relatively less efficient adhesive interaction than with the RBCs (lower incubation times with Caco-2 cells resulted in an immeasurably low binding for both wild-type and mutant bacteria – data not shown). Under these conditions, the adhesion level was fivefold higher for bacteria expressing fimbriae that incorporated CfaE with K201P and S244G point mutations. In keeping with flow chamber experiments with similarly modified CfaE and bovine RBCs, these bacteria thus showed increased Caco-2 cell binding in the absence of shear stress (Figs 7, S2A and B). The binding increase was likely due to the strengthening of individual CfaE

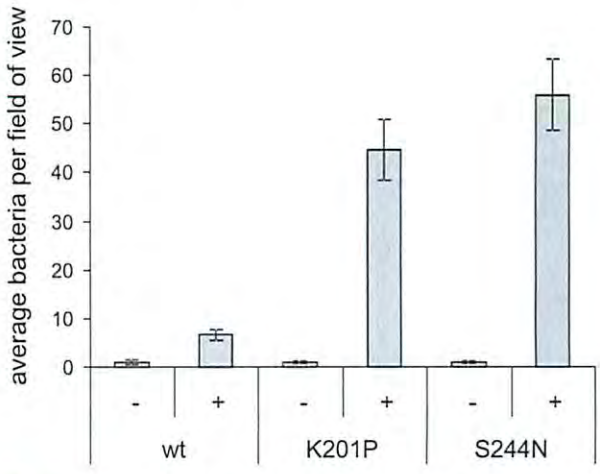

Fig. 7. Mutations in CfaE that shift the fimbrial binding of bovine erythrocytes in PPFC towards shear independency (K201P and S244N) increase bacterial binding to Caco-2 cells under static conditions. Isogenic *E. coli* were incubated with differentiated Caco-2 cells on slides. Bound bacteria were observed microscopically on stained slides; number of bound bacteria per field of view was calculated for 10 randomly chosen fields with uniform Caco-2 monolayer per each slide. Each condition was repeated twice on different slides; the average adhesion index (bacteria per field) was graphed with error bars representing standard error calculated for all fields. '–' and '+' indicate induction of fimbrial expression in bacteria.

bonds, as the amount of surface-expressed fimbriae and adhesin is similar for wild-type and mutant bacteria (Figs S1A and S2C). (We could not do the same experiment using bacteria with CfaE:G168D mutant, as this mutant has impaired CFA/I fimbrial expression – see above). The relative effect of mutations in CfaE is very similar between the bacterial binding to Caco-2 cells under static conditions and RBC binding to CFA/I fimbriae in a flow chamber at low shears within the 0.25–0.5 dynes cm^{-2} range. The RBC binding difference was less pronounced at the lowest shears, but the overall binding at those conditions was too low to measure accurately and the RBC incubation time in the flow chambers was much shorter (5 min) than of bacteria with the Caco-2 cells (3 h).

Thus, mutations in CfaE that were shown to increase binding of bovine erythrocytes by purified fimbria at lower shear stresses, also enabled bacteria to bind to Caco-2 cell receptor much more effectively under static conditions.

Discussion

In the present study we report several findings to indicate that CFA/I fimbriae of ETEC, through its adhesin CfaE, binds to erythrocytes in a shear-enhancing manner via a catch-bond mechanism of the ligand–receptor interaction. First, immobilized CFA/I fimbriae bind bovine and human erythrocytes in a shear-enhanced manner, which is characterized by weak or no binding (for bovine erythrocytes) or modest binding (for human erythrocytes) under static or low flow conditions, and a marked increase in erythrocyte adhesion to fimbriae at higher shear conditions. Second, the shear-enhanced binding pattern is replicated when the CFA/I fimbrial adhesin variant dscCfaE is immobilized to the chamber floor in place of CFA/I fimbriae. Lastly, the effect of shear-enhanced binding is based on a switch of the CfaEad between low- and high-affinity states, which appears to be allosterically regulated by interaction of its adhesin and pilin domains.

Catch bonds are defined as receptor–ligand bonds that are regulated by tensile mechanical force to become longer-lived (stronger) at higher forces (Isberg and Barnes, 2002; Marshall *et al.*, 2003). The existence of catch bonds in bacterial adhesive systems has been shown previously for FimH, the tip adhesin of type 1 fimbriae of *E. coli* (Thomas *et al.*, 2002; 2004; Nilsson *et al.*, 2006b). In PPFC experiments, type 1 fimbriated bacteria show shear-enhanced binding to mannosylated surfaces. Single-molecule studies have shown that this shear-enhanced binding results from catch bonding between the FimH adhesin and mannose, and that this is based on the ability of the adhesin to switch from a low-affinity to high-affinity conformational state (Tchesnokova *et al.*, 2008; Yakovenko *et al.*, 2008). It has been proposed that this switch is allosterically regulated by interaction between the binding (lectin) domain and fimbriae-incorporating (pilin) domain, wherein factors that disrupt the interdomain interactions (like stretching force, mutations that weaken interaction or molecules that wedge between domains) facilitate the switch from low- to high-affinity state of the binding domain.

The recently determined structure of the CfaE adhesin of CFA/I fimbriae revealed that it is composed of two tightly interacting domains (Li *et al.*, 2007). Because domain–domain interaction has been hypothesized (but not yet shown) to exist in FimH and to be the basis of its ability to form allosteric catch bonds (Aprikian *et al.*, 2007; Tchesnokova *et al.*, 2008), we investigated here whether CFA/I fimbriae mediate catch-bond adhesion. This was especially interesting as CFA/I fimbriae belong to class 5 fimbriae, which are genetically divergent from class 1 fimbriae (i.e., type 1 fimbriae). These two classes both feature fimbriae with stalks that consist of a polymerized major subunit assembled via the donor–strand complementation and exchange mechanism. However, class 1 fimbriae have a distinguishable tip fibrillum consisting of multiple minor adaptor subunits anchoring the adhesin to a pilus rod (Kuehn *et al.*, 1992; Jones *et al.*, 1995), whereas class 5 fimbriae have only an adhesive subunit and no adaptor proteins at the tip (Poole *et al.*, 2007; Mu *et al.*, 2008).

As mentioned above, the receptor for CFA/I fimbriae has yet to be defined and, thus, purified receptor analogue could not be used in the flow chamber tests as done previously for mannose-specific type 1 fimbriated bacteria (Thomas *et al.*, 2004). Instead, we established an inverted PPFC adhesion assay using a surface on which purified fimbriae had been immobilized, and flowed RBCs over this surface. Both the increase in binding at higher shear and its reversibility define the interaction between CFA/I fimbriae and RBCs as shear-dependent binding. The shear-dependent binding was obvious with both bovine and human erythrocytes, but most distinctly manifest with the former. It is quite possible that the human receptor structure is at least slightly different, mediating a generally stronger interaction with CfaE that would both increase the binding under low shears and lower the shear level of the binding peak. It is also possible that the receptor density could be much higher on human cells, which would increase the level of binding under lower shears.

The described shear-enhanced binding differs from that of FimH binding to mannose, as the erythrocytes never come to a complete stop on the CFA/I fimbrial carpet. This closely resembles shear-dependent selectin-mediated binding of leukocytes to LewisX oligosaccharide, where leukocytes move over the endothelial surface with hydro-

dynamic velocity at low shears, while above a shear threshold cells slow down significantly (Konstantopoulos *et al.*, 2003; Marshall *et al.*, 2003; Evans *et al.*, 2004; Sarangapani *et al.*, 2004; Yago *et al.*, 2004). It has recently been shown that selectin is capable of forming catch bonds with this ligand (Marshall *et al.*, 2002) and allosteric regulation has been invoked (Thomas *et al.*, 2006; Springer, 2009).

Other explanations besides formation of catch bonds have been suggested to explain the phenomenon of shear-enhanced adhesion, including an increased number of bonds formed between surfaces with multiple receptors. In that case, however, mutations that increase the binding under lower shears would be expected to increase the amount of adhesin expressed on the surface. As the fimbriation level is not increased in the shear-independent or -less-dependent CFA/I mutants (or even decreased in case of the G168D mutation), the shear-enhanced adhesion is most likely to be due to the functional changes in the adhesin, supporting the catch-bond properties of CfaE similar to ones of FimH. Also arguing against the binding increase because of the bond number increase is the reversibility of the strong binding to the weak one upon the drop in shear.

We have shown that purified CfaE is capable of shear-enhanced binding very similar to that observed with whole fimbriae, while the isolated CfaEad binds erythrocytes strongly at low shear. Similar findings have previously been shown for intact, two-domain FimH and its isolated lectin domain (Aprikian *et al.*, 2007). This suggests that: (i) the CfaE receptor binding domain can exist in two binding states, weak and strong and (ii) an intact, two-domain form of CfaE adhesin is capable of converting from the former to the latter under application of external tensile force, much like the catch-bond forming FimH protein. In support of this argument, mutations predicted to weaken interdomain interactions had the effect of enabling strong binding at lower shear force. We have previously shown that mutations in the FimH interdomain interface had similar effects on FimH binding to mannose (Aprikian *et al.*, 2007; Weissman *et al.*, 2007; Tchesnokova *et al.*, 2008).

In the SMD simulations of dscCfaE, upon application of external force the linker chain of CfaE (the 3/10-helix) was extended from the pilin domain, rather than from the adhesin domain as observed with FimH simulations where the extension has been proposed to serve as the trigger for the allosteric structural changes in the binding domain (Thomas *et al.*, 2002; Aprikian *et al.*, 2007). The linker extension from the pilin domain of CfaE, however, indicates that disruption of domain–domain interactions rather than deformation of linker loops directly influence the allosteric shift as was also proposed for FimH (Aprikian *et al.*, 2007; Tchesnokova *et al.*, 2008).

Presently, lack of knowledge on the defined CfaE receptor precludes single-molecule experiments by which one might directly test for catch-bond formation by CfaE, the tip-localized adhesin of CFA/I fimbriae. This limitation notwithstanding, the evidence presented herein is fully consistent with the interpretation that the shear-enhanced binding of erythrocytes to CfaE is due to catch-bond formation and that this mechanism is allosterically regulated via separation of the adhesin and pilin domains of CfaE. Shear-enhanced binding has been shown to facilitate the escape of type 1 fimbriated bacteria from the inhibitory effects of soluble ligand analogues, as FimH interactions with soluble ligands does not happen under shear (Nilsson *et al.*, 2006a). It has also been demonstrated that the ability of FimH to toggle between low- and high-affinity binding states enhances colonization of mannosylated surfaces by type 1 fimbriated *E. coli* (Anderson *et al.*, 2007), and serves as the initial step in formation of biofilms. Hence, catch-bond properties of fimbrial adhesins could provide some important advantages for the bacteria in colonization of their natural niches within the host.

Colonization factor antigen I and other class 5 fimbriae have been shown to be important for establishing infection in the human gut, where shear forces within 1–10 dynes cm^{-2} range are present because of the peristaltic movement (Jeffrey *et al.*, 2003; Lentle and Janssen, 2008). Findings presented here suggest that shear-enhanced binding could play a critical role in the interaction of CFA/I fimbriated bacteria with receptors on human tissues. Despite stronger interaction with receptors on human erythrocytes the shear-enhanced effect of this interaction is obvious. Moreover, bacteria that express CfaE with mutations that shift the binding mode towards shear independence are able to bind to Caco-2 cells much more effectively under static conditions.

We previously showed that immunization with the lectin domain of FimH produced antibodies against a ligand-induced binding site epitope in the FimH interdomain interface. When type 1 fimbriae were pretreated with an anti-ligand-induced binding site monoclonal antibody, enhancement of FimH binding to mannose was observed, with the antibody apparently wedging between the domains and locking the FimH lectin domain into its high-affinity state (Tchesnokova *et al.*, 2008). ETEC colonization factors have been a primary target in live-attenuated, killed whole-cell and purified subunit vaccine approaches, based on the proven role of CFA/I and related colonization factors as virulence determinants and protective antigens (Freedman *et al.*, 1998; Svennerholm and Tobias, 2008). Thus, our findings of catch-bond properties of CfaE bear some consideration in the vaccine research arena and illustrate the relevance of elucidating the basis for shear-

Table 1. Bacterial strains and plasmids used in this work.

Strain or plasmid	Description	Reference
E. coli		
H10407	ETEC severe diarrhea case isolate from Bangladesh (CFA/I; afimbrial adhesins EtpA and TibA; LTSTa; O78:H11)	Evans Jr and Evans (1973); Elsinghorst and Weitz (1994); Fleckenstein *et al.* (2006)
WS1933D	ETEC diarrhea isolate from Egypt (CFA/I; STa; O71:H45)	Shaheen *et al.* (2004)
BL21-SI	*E. coli* host [F⁻ *proUp*::T7RNAP::*malQ-lacZ ompT lon endA*1 *hsd*S_B(r_B^-, m_B^-) *gal dcm* Tc^s] used for cloning and overexpression of native and modified CFA/I fimbriae from the *proU* salt-inducible T7 RNA polymerase promoter	Gateway™, Life Technologies, Rockville, MD
BL21(DE3)	*E. coli* host [F⁻ *ompT* hsdS_B(r_B^-, m_B^-) *gal dcm* (DE3)] used for overexpression of variants of CFA/I fimbriae structural subunits	Invitrogen
Plasmids		
pET-24a(+)	T7 expression vector with C-terminal $(His)_6$ tag sequence; Kn^r; pBR322 *ori*	Novagen
pET24-*dsc_{19}cfaE[his]$_6$*	pET24a-based expression plasmid of dsc_{19}CfaE with C-terminal $(His)_6$ tag	Poole *et al.* (2007)
pET24-*cfaEad[his]$_6$*	pET24a-based plasmid for expression of CfaEad$(His)_6$ (or CfaEad), a genetically derived CfaE truncate comprising residues 1–202	This study
pMAM2	Expression vector pDEST14, modified by replacement of its ampicillin resistance (*bla*) with a kanamycin resistance (*aphA-3*) marker, with a cloning site insertion comprising the CFA/I bioassembly operon (*cfaABCE*)	Li *et al.* (2007)
pMAM2-CfaE/G168A	derivative of pMAM2 with point mutation that directs replacement of alanine for glycine at residue 168 of CfaE	This study
pMAM2-CfaE/G168D	derivative of pMAM2 with point mutation that directs replacement of aspartate for glycine at residue 168 of CfaE	This study
pMAM2-CfaE/K201P	derivative of pMAM2 with point mutation that directs replacement of proline for lysine at residue 201 of CfaE	This study
pMAM2-CfaE/S244G	derivative of pMAM2 with point mutation that directs replacement of glycine for serine at residue 244 of CfaE	This study
pMAM2-CfaE/S244N	derivative of pMAM2 with point mutation that directs replacement of asparaginine for serine at residue 244 of CfaE	This study

enhanced binding of CfaE and other class 5 ETEC adhesins to vaccine development.

Experimental procedures

Reagents and erythrocytes

All reagents were obtained from Sigma (St Louis, MO) unless stated otherwise. Bovine erythrocytes were purchased from Colorado Serum Company (Denver, CO) and were used within 3 weeks of the date of draw. Human type A erythrocytes were obtained from a volunteer donor.

Bacterial strains and plasmids

A list of bacterial strains and plasmids used or generated in this work is provided in Table 1. Unless otherwise indicated, bacteria were propagated on Luria–Bertani (LB) medium at 37°C. Antibiotics were added as needed at the following concentrations: ampicillin (Ap), 62.5 mg ml^{-1} and kanamycin (Kn), 50 mg ml^{-1}.

Site-directed mutagenesis

Single codon changes were introduced into the *cfaE* gene of pMAM2 by site-directed mutagenesis (Quikchange II, Stratagene) with specifically designed mutagenic primers, creating all of the derivatives shown in Table 1.

Fimbriae purification

Colonization factor antigen I whole fimbriae were purified as follows: bacterial strains were plated on LB agar plates with 300 mM NaCl and kanamycin (50 μg ml^{-1}) and grown overnight at 30°C. Bacteria were collected with cotton swab and inoculated in 2 l of LB broth, then grown overnight at 30°C with vigorous shaking. Bacteria were pelleted, and the pellet was resuspended in 20 mM Tris, pH 7.5, 150 mM NaCl buffer. Fimbriae were sheared off the cells using a PRO 200 Homogenizer (PRO Scientific, Oxford, CT, USA). Cell debris was removed by centrifugation; fimbriae were precipitated by 20% saturated ammonium sulphate, pelleted and resuspended in PBS pH 7.4, then dialysed against PBS and finally purified by size exclusion chromatography on Superdex 200 gel filtration column if required. Concentration of fimbrial proteins was determined using the BCA™ Protein Assay Kit (Pierce, Rockford, IL, USA). Fimbrial preparations were analysed by SDS-PAGE (Fig. S1A) and in ELISA (Fig. S1B) using polyclonal antibodies against whole CFA/I fimbriae and monoclonal antibodies against CfaE fimbrial tip adhesin. All fimbrial preparations yielded similar amounts of fimbriae in them, modified CfaE/G168D mutant (Fig. S1A). All fimbrial preparations were shown to have similar total fimbrial protein to CfaE adhesin ratio (Fig. S1B).

Cloning and purification of dscCfaE and a genetically derived truncate of the CfaEad

The engineering and cloning of dscCfaE have been described previously (Poole *et al.*, 2007). Briefly, dscCfaE contains a 19-residue C-terminal extension matching the N-terminus of mature CfaB, a portion of which forms a β-strand that fills a hydrophobic cleft in CfaE. Expression and purification of dscCfaE was carried by methods previously described (Poole *et al.*, 2007) with the following modifications. *E. coli* BL21(DE3)/pET24-*dsc*$_{19}$*cfaE[his]*$_6$ was grown in APS™ Superbroth with added glucose (5 mg per 100 ml) at 32°C, induced for 3 h by addition of 1 mM IPTG and harvested. After bacterial disruption by microfluidization and clarification by centrifugation, the supernatant was subject to a two-step process of nickel affinity chromatography using Ni-NTA Agarose Superflow resin (GE Healthcare Life Sciences) with a 50 mM imidazole wash step and a step gradient elution with 200 mM imidazole. Cation exchange was then performed using SP HiTrap HP resin (GE Healthcare Life Sciences) and step gradient elution with 200 mM NaCl.

The coding region for the adhesin domain of CfaE (codons 1–202) was amplified with custom primers by PCR from the template plasmid DNA made form ETEC wild-type strain H10407. This fragment was processed and cloned into the multi-cloning site of the expression plasmid pET-24a(+) in frame with the coding sequence for the C-terminal hexahistidine tag (see Table 1) and confirmed by DNA sequence analysis. The resulting plasmid pET24-*cfaEad[his]*$_6$ was transformed into *E. coli* BL21(DE3) and used for expression and purification of mature, signal-sequence cleaved CfaEad (residues 22–202). The strain was grown in APS™ Superbroth with 5 ml l^{-1} glycerol and induced in the late-logarithmic growth phase by addition of 1 mM IPTG for 3 h, all at 32°C. After bacterial disruption by microfluidization and centrifugation, CfaEad(His)$_6$ (subsequently called CfaEad) was purified by a two-step procedure involving nickel affinity chromatography using NiNTA HisTrap resin (GE Healthcare Life Sciences), and cation exchange chromatography using SP HiTrap resin (GE Healthcare, Life Sciences). Protein concentration of the final material was estimated by the BCA™ Protein Assay Kit (Pierce), and purity was shown to be 93%, as determined by densitometric analysis of a 15% SDS-PAGE gel.

Antibodies against dscCfaE

Mouse monoclonal antibodies (MAb) were produced against dscCfaE using standard methods as previously described (De Saint Groth and Scheidegger, 1980). One such antibody, MAb P10A7, was found to react to both dscCfaE and CfaEad by dot immunoblot analysis and ELISA, while another MAb P1F9 reacted with full-length CfaE but not CfaEad. Mutations in CfaE putative binding site (R181A, etc.) abolished binding of MAb P10A7 (α-CfaEad), but not MAb P1F9 (α-CfaE). Polyclonal R2175 anti-CFA/I antibodies were prepared by immunization of rabbit with purified CFA/I fimbria made from wild-type *E. coli* strain WS1933D with subsequent purification of polyclonal IgG by protein A affinity chromatography.

Flow chamber experiments

Polystyrene tissue culture plates were coated with proteins in 0.02 M $NaHCO_3$ buffer for 1 h at 37°C: fimbriae at 100 μg ml^{-1}, dscCfaE protein at 0.7 mg ml^{-1}, CfaEad at 0.35 mg ml^{-1}. Plates were quenched with 0.1 mg ml^{-1} of non-binding FimH mutant type 1 fimbriae preparation in 1× PBS to prevent non-specific binding of bovine erythrocytes to BSA. To test the effect of antibodies they were added at 1:100 dilution in 1× PBS in the presence of the same non-binding type 1 fimbrial solution and incubated for 3 h at 37°C. Then a 2.5 cm × 0.25 cm × 250 μm PPFC (GlycoTech) was assembled over the plates according to manufacturer. The assembly was mounted on a Nikon TE200 inverted microscope with a 10× phase-contrast objective. Experiments were recorded using a Roper Scientific high-resolution CCD camera and MetaMorph® or MetaView® (Universal Imaging Corporation™) video acquisition software. All further experiments were performed in 0.2% BSA-PBS buffer with 0.5% α-methyl D-mannopyrannoside. Bovine erythrocytes were washed at least twice and resuspended at 0.04%.

Accumulation experiments

Erythrocyte suspensions were manually loaded into assembled PPFC and allowed to settle for 4 min. The recording was started, and buffer was pushed into the chamber using a Harvard syringe pump at various flow rates to produce the desired wall shear rates. Erythrocyte movement was recorded at two frames per second with 100 ms shutter time to distinguish cells that are moving with velocities slower than hydrodynamic speed. Time of recording varied depending on the period of delay for each shear rate. Recorded movies were analysed as follows: settled red cells were counted before the flow was turned on. Then, after flow in the chamber was established, erythrocytes that were in focus (moving slower than the ones that were moving with hydrodynamic speed) were counted on several sequential frames. These counts were used to calculate the average percent of red cells that stayed near the surface (i.e., bound erythrocytes). Each experiment was repeated at least two times using different protein and erythrocytes batches.

Erythrocyte velocities

To determine the velocities of moving erythrocytes, the same setup was used as for accumulation experiments, but the recording was made in stream video mode (1 frame per 37 ms) if needed. Velocity of each individual cell was calculated using the tracking object mode of Metamorph software, when possible, or manually, evaluating the distance covered by the erythrocyte within a given time period. The velocity of every cell in the field of view was determined, and the average velocity with standard errors was calculated from the velocities of approximately 100 cells within the same video.

Steered molecular dynamics

Steered molecular dynamics was performed using the software package NAMD (Phillips *et al.*, 2005) and the all-atom

force field AMBER (Duan *et al.*, 2003). NAMD was developed by the Theoretical and Computational Biophysics Group in the Beckman Institute for Advanced Science and Technology at the University of Illinois at Urbana-Champaign. The initial conformation of CfaE was taken from the co-ordinates deposited in the protein data bank [pdb code: 2hb0 (Li *et al.*, 2007)]. TIP3P (Mahoney and Jorgensen, 2000) water molecules were placed around the protein with a minimum distance of 10 Å between the protein and the edge of the box in every direction. The starting dimensions of the parallelepiped box were 155 Å × 61 Å × 58 Å. Counter ions of sodium and chlorine were added to neutralize the system and simulate a physiological salt concentration of 0.15 M. Short-range electrostatics were computed with a non-bonded pair list cut-off of 10 Å. Electrostatic interactions beyond 10 Å were calculated using the particle-mesh Ewald method (Darden *et al.*, 1993). Non-bonded van der Waals interactions were calculated using a switching function that started at 8 Å and turned off at 10 Å. A time step of 2 fs was used for numerical integration and the bond lengths of hydrogen atoms were constrained using the SHAKE algorithm with a tolerance of 5×10^{-4}.

The starting conformation was minimized in 6000 steps, using the conjugate gradient method. Following minimization, the system was heated over 40 ps by increasing the temperature in step-increments of 10 K every 1.0 ps and holding constant at the target of 300 K. The temperature was kept constant by coupling the system to an external thermal bath of 300 K (Berendsen *et al.*, 1984), while the pressure was held at constant by coupling to a piston set at 1 bar with a time constant of 1.0 ps. Prior to pulling, an equilibration simulation was run for 4 ns. SMD was performed by fixing the Cα atom of the C-terminus (V378) and pulling the centre of mass of the adhesin domain (Cα atoms of residues A23-D200) at a constant velocity of $v = 2.5$ Å ns^{-1}, using a spring constant of $\kappa = 139$ pN Å^{-1}.

Bacterial adhesion to Caco-2 human intestinal epithelial cells

Caco-2 cells were seeded in 12-well plates loaded with tissue culture-treated glass slides and grown for 14–16 days to differentiate in DMEM medium supplemented with penicillin/streptomycin, 10% fetal bovine serum, 4 mM L-glutamine and 0.1 mM non-essential aminoacids. Isogenic *E. coli* expressing CFA/I fimbriae with different CfaE adhesins (BL21-SI with various pMAM2's) were seeded from fresh LBON agar plates (no NaCl to prevent fimbrial expression) into LB or LBON broth supplemented with 50 μg ml^{-1} kanamycin and grown overnight at 30°C with vigorous shaking. Grown bacteria were washed with PBS and resuspended in DMEM to OD 10.0 (2.5×10^9 cfu ml^{-1}) and 1.0 (2.5×10^8 cfu ml^{-1}). Bacteria at OD 10.0 were used to check the bovine and human RBC agglutination to determine the CFA/I fimbria expression on them; same bacterial suspension was used to analyse CfaE expression by SDS-PAGE and Western blot analyses. Differentiated Caco-2 cell slides in wells were washed with DMEM medium; 2 ml of bacterial suspension was added to each well and incubated for 3 h at 37°C in 5% CO2. Unbound bacteria were washed away, slides were fixed, and cells were stained using HEMA 3® staining kit (Protocol, Kalamazoo, MI). Bound bacteria were observed microscopically: for each slide, 10 random fields of view with uniform Caco-2 cells monolayer were examined and bound bacterial cells were counted giving the adhesion index of bacteria per field of view. The experiments were repeated several times with duplicates of every condition. When GFP-labelled bacteria were used, slides were fixed with 4% paraformaldehyde for 10 min, rinsed with PBS and mounted, and then visualized on the same microscope that was used for PPFC experiments using 20× magnification lens. First, slides were examined under transmitted light, to choose the spots with intact monolayer, then bound GFP-expressing bacterial cells were recorded. Images of eight fields were taken for each slide; slides were prepared in duplicates.

Acknowledgements

We gratefully acknowledge Pavel Aprikian and Natalia Korotkova for critical advice and Sami Farid for producing key reagents (anti-CfaE monoclonal antibodies). This work was supported by the National Institutes of Health, R01 AI050940 (to E.V.S.), the US Army, MIDRP Work Unit A0307 (to S.J.S.), the Henry M. Jackson Foundation for the Advancement of Military Medicine (S.J.S.). The views expressed in this article are those of the authors and do not necessarily reflect the official position of the Department of the Navy, Department of Defense, nor the US Government.

References

Anantha, R.P., McVeigh, A.L., Lee, L.H., Agnew, M.K., Cassels, F.J., Scott, D.A., *et al.* (2004) Evolutionary and functional relationships of colonization factor antigen i and other class 5 adhesive fimbriae of enterotoxigenic *Escherichia coli*. *Infect Immun* **72:** 7190–7201.

Anderson, B.N., Ding, A.M., Nilsson, L.M., Kusuma, K., Tchesnokova, V., Vogel, V., *et al.* (2007) Weak rolling adhesion enhances bacterial surface colonization. *J Bacteriol* **189:** 1794–1802.

Aprikian, P., Tchesnokova, V., Kidd, B., Yakovenko, O., Yarov-Yarovoy, V., Trinchina, E., *et al.* (2007) Interdomain interaction in the FimH adhesin of *Escherichia coli* regulates the affinity to mannose. *J Biol Chem* **282:** 23437–23446.

Baker, K.K., Levine, M.M., Morison, J., Phillips, A., and Barry, E.M. (2009) CfaE tip mutations in ETEC CFA/I fimbriae define critical human intestinal binding sites. *Cell Microbiol* **11:** 742–754.

Bartus, H., Actor, P., Snipes, E., Sedlock, D., and Zajac, I. (1985) Indications that the erythrocyte receptor involved in enterotoxigenic *Escherichia coli* attachment is a sialoglycoconjugate. *J Clin Microbiol* **21:** 951–954.

Berendsen, H.J.C., Postma, J.P.M., van Gunsteren, W.F., DiNola, A., and Haak, J.R. (1984) Molecular dynamics with coupling to an external bath. *J Chem Phys* **81:** 3684–3690.

Darden, T., York, D., and Pedersen, L. (1993) Particle mesh Ewald: An N·log(N) method for Ewald sums in large systems. *J Chem Phys* **98:** 10089–10092.

Darfeuille-Michaud, A., Aubel, D., Chauviere, G., Rich, C., Bourges, M., Servin, A., and Joly, B. (1990) Adhesion of enterotoxigenic *Escherichia coli* to the human colon carci-

noma cell line Caco-2 in culture. *Infect Immun* **58:** 893–902.

De Saint Groth, S.F., and Scheidegger, D.J. (1980) Production of monoclonal antibodies: strategies and tactics. *J Immunol Methods* **35:** 1–21.

Duan, Y., Wu, C., Chowdhury, S., Lee, M.C., Xiong, G., Zhang, W., *et al.* (2003) A point-charge force field for molecular mechanics simulations of proteins based on condensed-phase quantum mechanical calculations. *J Comput Chem* **24:** 1999–2012.

Elsinghorst, E.A., and Weitz, J.A. (1994) Epithelial cell invasion and adherence directed by the enterotoxigenic *Escherichia coli* tib locus is associated with a 104-kilodalton outer membrane protein. *Infect Immun* **62:** 3463–3471.

Evans, D.G., Silver, R.P., Evans, D.J., Jr, Chase, D.G., and Gorbach, S.L. (1975) Plasmid-controlled colonization factor associated with virulence in Esherichia coli enterotoxigenic for humans. *Infect Immun* **12:** 656–667.

Evans, D.G., Evans, D.J., Jr, Clegg, S., and Pauley, J.A. (1979) Purification and characterization of the CFA/I antigen of enterotoxigenic *Escherichia coli*. *Infect Immun* **25:** 738–748.

Evans, D.J., Jr, and Evans, D.G. (1973) Three characteristics associated with enterotoxigenic *Escherichia coli* isolated from man. *Infect Immun* **8:** 322–328.

Evans, E., Leung, A., Heinrich, V., and Zhu, C. (2004) Mechanical switching and coupling between two dissociation pathways in a P-selectin adhesion bond. *Proc Natl Acad Sci USA* **101:** 11281–11286.

Fleckenstein, J.M., Roy, K., Fischer, J.F., and Burkitt, M. (2006) Identification of a two-partner secretion locus of enterotoxigenic *Escherichia coli*. *Infect Immun* **74:** 2245–2258.

Freedman, D.J., Tacket, C.O., Delehanty, A., Maneval, D.R., Nataro, J., and Crabb, J.H. (1998) Milk immunoglobulin with specific activity against purified colonization factor antigens can protect against oral challenge with enterotoxigenic *Escherichia coli*. *J Infect Dis* **177:** 662–667.

Gaastra, W., and Svennerholm, A.M. (1996) Colonization factors of human enterotoxigenic *Escherichia coli* (ETEC). *Trends Microbiol* **4:** 444–452.

Gaastra, W., Sommerfelt, H., van Dijk, L., Kusters, J.G., Svennerholm, A.M., and Grewal, H.M. (2002) Antigenic variation within the subunit protein of members of the colonization factor antigen I group of fimbrial proteins in human enterotoxigenic *Escherichia coli*. *Int J Med Microbiol* **292:** 43–50.

Isberg, R.R., and Barnes, P. (2002) Dancing with the host; flow-dependent bacterial adhesion. *Cell* **110:** 1–4.

Jeffrey, B., Udaykumar, H.S., and Schulze, K.S. (2003) Flow fields generated by peristaltic reflex in isolated guinea pig ileum: impact of contraction depth and shoulders. *Am J Physiol Gastrointest Liver Physiol* **285:** G907–G918.

Jones, C.H., Pinkner, J.S., Roth, R., Heuser, J., Nicholes, A.V., Abraham, S.N., and Hultgren, S.J. (1995) FimH adhesin of type 1 pili is assembled into a fibrillar tip structure in the Enterobacteriaceae. *Proc Natl Acad Sci USA* **92:** 2081–2085.

Jordi, B.J., Willshaw, G.A., van der Zeijst, B.A., and Gaastra, W. (1992) The complete nucleotide sequence of region 1 of the CFA/I fimbrial operon of human enterotoxigenic *Escherichia coli*. *DNA Seq* **2:** 257–263.

Konstantopoulos, K., Hanley, W.D., and Wirtz, D. (2003) Receptor-ligand binding: 'catch' bonds finally caught. *Curr Biol* **13:** R611–R613.

Kuehn, M.J., Heuser, J., Normark, S., and Hultgren, S.J. (1992) P pili in uropathogenic *E. coli* are composite fibres with distinct fibrillar adhesive tips. *Nature* **356:** 252–255.

Lentle, R.G., and Janssen, P.W. (2008) Physical characteristics of digesta and their influence on flow and mixing in the mammalian intestine: a review. *J Comp Physiol [B]* **178:** 673–690.

Levine, M.M. (1987) *Escherichia coli* that cause diarrhea: enterotoxigenic, enteropathogenic, enteroinvasive, enterohemorrhagic, and enteroadherent. *J Infect Dis* **155:** 377–389.

Li, Y.F., Poole, S., Rasulova, F., McVeigh, A.L., Savarino, S.J., and Xia, D. (2007) A receptor-binding site as revealed by the crystal structure of CfaE, the colonization factor antigen I fimbrial adhesin of enterotoxigenic *Escherichia coli*. *J Biol Chem* **282:** 23970–23980.

Mahoney, M.W., and Jorgensen, L.W. (2000) A five-site model for liquid water the reproduction of the density anomaly by rigid, nonpolarizable potential. *J Chem Phys* **112:** 8910–8922.

Marshall, B.T., McEver, R.P., and Zhu, C. (2002) Mechanical properties of the P-selectin/PSGL-1 interaction. In *Second Joint EBMS/BMES Conference*, Vol. 3. Houston, TX: IEEE, pp. 337–338.

Marshall, B.T., Long, M., Piper, J.W., Yago, T., McEver, R.P., and Zhu, C. (2003) Direct observation of catch bonds involving cell-adhesion molecules. *Nature* **423:** 190–193.

Mu, X.Q., Savarino, S.J., and Bullitt, E. (2008) The three-dimensional structure of CFA/I adhesion pili: traveler's diarrhea bacteria hang on by a spring. *J Mol Biol* **376:** 614–620.

Nilsson, L.M., Thomas, W.E., Sokurenko, E.V., and Vogel, V. (2006a) Elevated shear stress protects *Escherichia coli* cells adhering to surfaces via catch bonds from detachment by soluble inhibitors. *Appl Environ Microbiol* **72:** 3005–3010.

Nilsson, L.M., Thomas, W.E., Trintchina, E., Vogel, V., and Sokurenko, E.V. (2006b) Catch bond-mediated adhesion without a shear threshold: trimannose versus monomannose interactions with the FimH adhesin of *Escherichia coli*. *J Biol Chem* **281:** 16656–16663.

Phillips, J.C., Braun, R., Wang, W., Gumbart, J., Tajkhorshid, E., Villa, E., *et al.* (2005) Scalable molecular dynamics with NAMD. *J Comput Chem* **26:** 1781–1802.

Poole, S.T., McVeigh, A.L., Anantha, R.P., Lee, L.H., Akay, Y.M., Pontzer, E.A., *et al.* (2007) Donor strand complementation governs intersubunit interaction of fimbriae of the alternate chaperone pathway. *Mol Microbiol* **63:** 1372–1384.

Sakellaris, H., Balding, D.P., and Scott, J.R. (1996) Assembly proteins of CS1 pili of enterotoxigenic *Escherichia coli*. *Mol Microbiol* **21:** 529–541.

Sarangapani, K.K., Yago, T., Klopocki, A.G., Lawrence, M.B., Fieger, C.B., Rosen, S.D., *et al.* (2004) Low force decelerates l-selectin dissociation from P-selectin glycoprotein ligand-1 and endoglycan. *J Biol Chem* **279:** 2291–2298.

Shaheen, H.I., Khalil, S.B., Rao, M.R., Abu Elyazeed, R., Wierzba, T.F., Peruski, L.F., Jr, *et al.* (2004) Phenotypic profiles of enterotoxigenic *Escherichia coli* associated with early childhood diarrhea in rural Egypt. *J Clin Microbiol* **42:** 5588–5595.

Springer, T.A. (2009) Structural basis for selectin mechanochemistry. *Proc Natl Acad Sci USA* **106:** 91–96.

Svennerholm, A.M., and Tobias, J. (2008) Vaccines against enterotoxigenic *Escherichia coli. Expert Rev Vaccines* **7:** 795–804.

Tchesnokova, V., Aprikian, P., Yakovenko, O., Larock, C., Kidd, B., Vogel, V., *et al.* (2008) Integrin-like allosteric properties of the catch bond-forming FimH adhesin of *Escherichia coli. J Biol Chem* **283:** 7823–7833.

Thomas, W.E., Trintchina, E., Forero, M., Vogel, V., and Sokurenko, E.V. (2002) Bacterial adhesion to target cells enhanced by shear force. *Cell* **109:** 913–923.

Thomas, W.E., Nilsson, L., Forero, M., Sokurenko, E.V., and Vogel, V. (2004) 'Stick-and-roll' bacterial adhesion mediated by catch-bonds. *Mol Microbiol* **53:** 1545.

Thomas, W.E., Forero, M., Yakovenko, O., Nilsson, L., Vicini, P., Sokurenko, E.V., and Vogel, V. (2006) Catch bond model derived from allostery explains force-activated bacterial adhesion. *Biophys J* **90:** 753–764.

Weissman, S.J., Beskhlebnaya, V., Chesnokova, V., Chattopadhyay, S., Stamm, W.E., Hooton, T.M., and Sokurenko, E.V. (2007) Differential stability and trade-off effects of pathoadaptive mutations in the *Escherichia coli* FimH adhesin. *Infect Immun* **75:** 3548–3555.

Yago, T., Wu, J., Wey, C.D., Klopocki, A.G., Zhu, C., and McEver, R.P. (2004) Catch bonds govern adhesion through l-selectin at threshold shear. *J Cell Biol* **166:** 913–923.

Yakovenko, O., Sharma, S., Forero, M., Tchesnokova, V., Aprikian, P., Kidd, B., *et al.* (2008) FimH forms catch bonds that are enhanced by mechanical force due to allosteric regulation. *J Biol Chem* **283:** 11596–11605.

Supporting information

Additional supporting information may be found in the online version of this article.

Please note: Wiley-Blackwell are not responsible for the content or functionality of any supporting materials supplied by the authors. Any queries (other than missing material) should be directed to the corresponding author for the article.